HHS Public Access

Nanocrystal dispersion of DK-I-56–1, a poorly soluble pyrazoloquinolinone positive modulator of α6 GABA_A receptors: formulation approach toward improved *in vivo* performance

Jelena R. Mitrovi [a], Branka Divovi [b], Daniel E. Knutson[c], Jelena B. okovi [d], Predrag J. Vuli [e], Danijela V. Randjelovi [f], Vladimir D. Dobri i [g], Bojan R. alija[h], James M. Cook[i], Miroslav M. Savi [j], Snežana D. Savi [k,*]

[a]Department of Pharmaceutical Technology and Cosmetology, Faculty of Pharmacy, University of Belgrade, Vojvode Stepe 450, 11221 Belgrade, Serbia.

[b]Department of Pharmacology, Faculty of Pharmacy, University of Belgrade, Vojvode Stepe 450, 11221 Belgrade, Serbia.

[c]Department of Chemistry and Biochemistry, Milwaukee Institute for Drug Discovery, University of Wisconsin-Milwaukee, 3210 N. Cramer St., Milwaukee, Wisconsin 53211, United States.

[d]Department of Pharmaceutical Technology and Cosmetology, Faculty of Pharmacy, University of Belgrade, Vojvode Stepe 450, 11221 Belgrade, Serbia.

[e]Laboratory of Crystallography, Faculty of Mining and Geology, University of Belgrade, ušina 7, 11000 Belgrade, Serbia.

[f]Department of Microelectronic Technologies, Institute of Chemistry, Technology and Metallurgy, University of Belgrade, Njegoševa 12, 11000 Belgrade, Serbia.

[g]Department of Pharmaceutical Chemistry, Faculty of Pharmacy, University of Belgrade, Vojvode Stepe 450, 11221 Belgrade, Serbia.

[h]Department of Pharmaceutical Technology and Cosmetology, Faculty of Pharmacy, University of Belgrade, Vojvode Stepe 450, 11221 Belgrade, Serbia.

[i]Department of Chemistry and Biochemistry, Milwaukee Institute for Drug Discovery, University of Wisconsin-Milwaukee, 3210 N. Cramer St., Milwaukee, Wisconsin 53211, United States.

*Corresponding author: Dr Snežana Savi , Department of Pharmaceutical Technology and Cosmetology, Faculty of Pharmacy, University of Belgrade, Vojvode Stepe 450, 11221 Belgrade, Serbia, Tel.: +381-11-3951288; Fax: +381-11-3972840, snezana.savic@pharmacy.bg.ac.rs.

Declaration of Competing Interest
Declarations of interest: none.

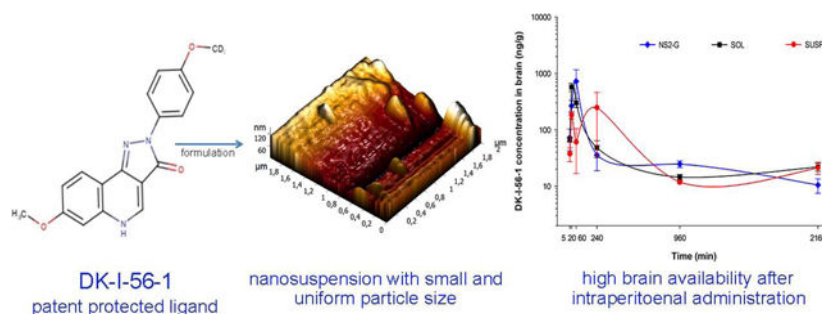jDepartment of Pharmacology, Faculty of Pharmacy, University of Belgrade, Vojvode Stepe 450, 11221 Belgrade, Serbia.

kDepartment of Pharmaceutical Technology and Cosmetology, Faculty of Pharmacy, University of Belgrade, Vojvode Stepe 450, 11221 Belgrade, Serbia.

Abstract

DK-I-56–1 (7-methoxy-2-(4-methoxy-d_3-phenyl)-2,5-dihydro-$3H$-pyrazolo[4,3-c]quinolin-3-one), a recently developed deuterated pyrazoloquinolinone, has been recognized as a lead candidate for treatment of various neuropsychiatric disorders. During preclinical investigation of poorly water-soluble compounds such as DK-I-56–1, the application of nanotechnology could be advantageous due to improved safety and possibly increased bioavailability of nanosized formulation. DK-I-56–1 nanosuspensions stabilized by polysorbate 80, alone or in combination with poloxamers 188 i.e. 407 or d-α-tocopheryl polyethylene glycol 1000 succinate, were prepared using a small-scale media milling device. With particle size 208.7–250.6 nm and polydispersity index <0.250, selected nanodiseprsions were stable for three weeks. Pharmacokinetic and biodistribution studies following intraperitoneal administration of three types of formulation in mice indicated high plasma DK-I-56–1 levels after solution (10228.6 ± 1037.2 ngh/ml) and nanosuspension (6770.4 ± 770.7 ngh/ml) but not suspension administration (966.0 ± 58.1 ngh/ml). However, distribution of DK-I-56–1 after solution was heavily influenced by its composition, and brain availability of nanosuspension was superior to that of solution formulation. In spontaneous locomotor activity test, the expected hyperlocomotor effect was observed after nanosuspension administration, without compromising impact of the vehicle/excipients used. Therefore, nanonization of drug compound assembled with proper selection of stabilizers may seemingly contribute further thorough testing of DK-I-56–1 preclinical efficacy.

Graphical

Graphical Abstract

DK-I-56-1
patent protected ligand

nanosuspension with small and
uniform particle size

high brain availability after
intraperitoenal administration

Keywords

pyrazoloquinolinones; nanosuspension; wet ball milling; pharmacokinetics; biodistribution; pharmacodynamics

1. Introduction

Novel patent-protected deuterated pyrazoloquinolinones, and especially DK-I-56–1 (7-Methoxy-2-(4-methoxy-d_3-phenyl)-2,5-dihydro-3H-pyrazolo[4,3-c]quinolin-3-one), have potential therapeutic use in a number of psychiatric and neurological disorders in which disbalance of GABAergic neurotransmission takes place (Chiou et al., 2018a; Chiou et al., 2018b; Fan et al., 2018; Knutson et al., 2018; Vasovi et al., 2019). They act as positive allosteric modulators of benzodiazepine-insensitive $\alpha6\beta2/3\gamma2$ subtype of $GABA_A$ receptors, and null modulators at the benzodiazepine binding site, thus causing no undesired effects such as sedation. However, while hydrogen-to-deuterium substitution on C4' in DK-I-56–1 molecule improves metabolic stability (Knutson et al., 2018), poor solubility still hinders its systemic administration.

Unfavorable physicochemical characteristics of drug candidates are recognized as one of the main obstacles in drug discovery and development (Grohganz et al., 2014), with estimation that approximately 75% of compounds under development are poorly water-soluble (Williams et al., 2013). Nevertheless, development of a formulation that enables acceptable systemic exposure is a necessary prerequisite for early pharmacology and toxicology preclinical studies (Ayad, 2015). For poorly soluble substances, parenteral administration of a solution formulation is not possible without using high concentrations of organic solvents and/or surfactants, which increases odds of vehicle-related safety issues (Gao et al., 2010; Pestel et al., 2006). Furthermore, administration of microsuspensions, although applicable for intraperitoneal (i.p.) route of administration as a frequent choice in early drug discovery, usually results in low drug levels in plasma (Müller et al., 2001). One of the strategies to overcome these problems is substance 'nanonization', i.e. reducing particle size to sub-micron range (Kalepu and Nekkanti, 2015).

Growing interest for nanosuspension formulation is reflected in fact that 30% of all FDA applications in 2017 for nanomaterial-containing drug products involved nanocrystals (Chen et al., 2017). Nanosuspensions, or more precisely nano-crystalline suspensions, are dispersions of nanocrystals with particle size bellow 1000 nm, which tends to improve physicochemical properties of drug substances such as saturation solubility and dissolution. However, due to large surface area and high surface energy, nanocrystal particles are prone to aggregate during storage, which can compromise both, their advantages as nanoparticulate systems and their safety (Wu et al., 2011). Typically, surfactants and polymers in a wide range of concentrations, as well as their combinations, are used for nanosuspension stabilization (Van Eerdenbrugh et al., 2008). The type and concentration of stabilizers are critical formulation parameters affecting nanosuspension quality and stability, and as such need to be carefully examined (Chin et al., 2014; George and Ghosh, 2013; Van Eerdenbrugh et al., 2009; Wang et al., 2013).

Nanosuspensions can be obtained by two main techniques – bottom-up (controlled precipitation or crystallization) and top-down (particle size reduction by mechanical attrition), with the latter ones being preferable for scaling up to industrial level (Shegokar and Müller, 2010; Müller et al., 2011). Two kinds of top-down methods were introduced: wet media milling and high pressure homogenization. During nanonization using wet media

milling techniques, energy generated from the collision of the drug and milling media is used for chopping the particles to a desired size (Liu et al., 2015). With increasing interest for nanosuspensions formulation during early phases of drug development, a lot of effort is put to miniaturize production process (Frank and Boeck, 2016; Van Eerdenbrugh et al., 2008). One of the approaches is using cell disruptor device, with yttrium-stabilized zirconium beads as milling media (Corrias et al., 2017).

Submicron particle size makes nanosuspensions suitable for both systemic routes of administration – oral and parenteral (Shegokar and Müller, 2010). In preclinical studies in rodents, intraperitoneal route of administration is commonly applied, due to safe use of relatively large volumes (Turner et al., 2011), and less strict limitations regarding particle size than for intravenous administration (Shekunov et al., 2007). Thus, nanosuspension formulation could be considered as a promising tool to overcome unfavorable DK-I-56–1 physicochemical properties in preclinical investigation. Therefore, we aimed to develop nanosuspensions of DK-I-56–1, with satisfactory stability intended for preclinical studies, using small scale wet ball milling technique. Comprehensive physicochemical characterization, including particle size measurements and solid-state investigation, was carried out in order to analyze their suitability for parenteral administration and check for possible changes of DK-I-56–1 crystallinity during milling. Finally, developed nanosuspensions were examined *in vivo* on mice subjected to pharmacokinetic and behavioral studies, to elucidate the feasibility of this type of drug formulation for appropriate preclinical evaluation.

2.   Materials and Methods

2.1.   Materials

DK-I-56–1 was synthesized at the Department of Chemistry and Biochemistry, University of Wisconsin—Milwaukee, USA (Knutson et al., 2018). The following other materials were used: medium chain triglycerides, propylene glycol (Fagron GmbH & KG, Germany), soybean oil (Lipoid Purified Soybean Oil 700, Lipoid GmbH, Germany), castor oil, fish oil, isopropanol, benzyl alcohol, polysorbate 80, poloxamer 188, d-α-tocopheryl polyethylene glycol 1000 succinate (Sigma-Aldrich Laborchemikalien GmbH, Germany), methanol, ethanol, dimethyl sulfoxide (Fisher scientific, UK), poloxamer 407, Cremophor EL (BASF Ludwigshafen, Germany), glycerol,   98% (Carl Roth GmbH, Germany). Fresh ultrapure water was supplied from a TKA GenPure system (TKA Wasseranfbereitungssysteme GmbH, Germany).

2.2.   Solubility study

Solubility of DK-I-56–1 in selected solvents was examined by shake-flask method. Excess amount of DK-I-56–1 was added to: water; medium chain triglycerides; soybean oil; castor oil; fish oil; isopropanol; methanol; ethanol, 70% v/v; dimethyl sulfoxide (DMSO) and benzyl alcohol, as well as stabilizer solutions (0.2%, 0.1% and 0.05% polysorbate 80, 0.05% poloxamer 188, 0.05% poloxamer 407 and 0.05% d-α-tocopheryl polyethylene glycol 1000 succinate (TPGS)). After mixing the samples on vortex during 24 h at the temperature 25

± 2 °C, they were centrifuged (1000 × g, 10 min, 25 °C) on MiniSpin® plus centrifuge (Eppendorf, Germany), diluted in isopropanol and analyzed using LC-MS/MS method.

2.3. Nanosuspension preparation

Nanocrystal dispersions were prepared by modified wet ball milling technique. DK-I-56–1 (0.2% w/w) was dispersed in aqueous stabilizer solution and homogenized on rotor stator homogenizer IKA Ultra-Turrax® T25 digital (IKAR-Werke GmbH & Company KG) for 5 min at 10000 rpm. For nanosuspensions stabilized by polysorbate 80 alone (formulations NS1, NS2 and NS3), its concentration was 25%, 50% and 100%, respectively, relative to DK-I-56–1 concentration. In nanosuspensions stabilized by combination of polysorbate 80 and poloxamer 407, poloxamer 188 or TPGS (NS4, NS5 and NS6, respectively), total surfactant concentration was 50% of DK-I-56–1 concentration (polysorbate 80: second stabilizer 1:1). The dispersion was then separated to 2-ml tubes containing 60% v/v 0.1–0.2 mm yttrium stabilized zirconium beads (SiLibeads® Typ ZY-S, Sigmund Lindner, Germany) and shaken for 1 h using a beads-milling cell disruptor equipment (Disruptor Genie, Scientific Industries, USA). Afterwards, obtained portions of nanosuspension were separated from beads and gathered in glass bottles. Suspension (S2) with same composition as NS2 (physical mixture) was prepared on magnetic stirrer (RH basic 2 IKAMAGR Magnetic Stirrer; IKAR -Werke GmbH & Company KG) at 25 °C. This suspension was used for DSC, XRPD and dissolution studies. Formulations were stored in crimped glass bottles at 25 ± 2 °C for three weeks.

2.4. Particle size measurements

The mean particle size (intensity weighted mean diameter, z-ave) and particle size distribution (PDI) of nanosuspensions were determined by dynamic light scattering (DLS) using a Zetasizer Nano ZS90 (Malvern Instruments Ltd., Worcestershire, UK). Before measurements, samples were diluted with ultrapure water 1:100 (v/v). Measurements were performed at predetermined time intervals (1h, 1 and 21 days after preparation), and each measurement was done in triplicates with results presented as mean ± S.D. Laser diffractometry (LD) was used as additional method for particle sizing. Measurements were performed using the mastersizer instrument (Malvern Mastersizer 3000 equipped with a Hydro EV dispersion cell, Malvern, Instruments Ltd., UK). Measurements were performed in 200 ml purified water as dispersant medium, with stirring speed of 2000 rpm. For calculating particle size, a refractive index of 1.4 was used. Results were expressed as D(v, 0.1), D(v, 0.5) and D(v, 0.9) values (10%, 50% or 90% of the particle volume below a particular size, respectively). For statistical analysis, one-way ANOVA with Tukey HSD as post hoc was used, with $P<0.05$ as statistically significant.

2.5. Atomic force microscopy

Surface topography and profiles of the selected nanosuspension (NS2) were observed using NTEGRA prima atomic force microscope (NT-MDT). 10 μl of undiluted or diluted (1:100 v/v) NS2 was placed on the circular mica substrate (Highest Grade V1 AFM Mica Discs, Ted Pella Inc., Redding, California, USA) and dried in vacuum dryer for 30 min at 25 °C. Measurements were carried out in air using intermittent-contact AFM mode. For this purpose, NT-MDT NSGO1 silicon cantilevers (N-type, Antimony doped, Au reflective

coating) were used. Nominal force constant of these cantilevers is 5.1 N/m. During the measurements cantilever driving frequency was around 150 kHz. Both topography and "error signal" AFM images were taken, and later analyzed using the software Image Analysis 2.2.0 (NT-MDT).

2.6. Zeta potential measurements

The particle surface charge of selected nanosuspensions was determined using Zetasizer Nano ZS90 (Malvern Instruments Ltd., UK). Zeta potential (ZP) measurements were performed at 25 °C after dilution in ultrapure water 1:100 (v/v), the conductivity of which was adjusted to 50 μS/cm by sodium chloride. Measurements were performed in triplicates and results are expressed as mean ± S.D.

2.7. Physical state evaluation

2.7.1.　Sample preparation—Samples were prepared in a similar way to the procedure described by Ali et al. (2011). Nanosuspension and suspension formulations were centrifuged on MiniSpin® plus centrifuge (Eppendorf, Germany) at $1000 \times g$ for 10 min, and after supernatant removal dried for 24 h at 25 °C in vacuum drying oven VT 6025 (Thermo Heraeus, Fisher Scientific, UK).

2.7.2.　Differential scanning calorimetry (DSC)—Samples (around 2 mg) were measured in aluminum pans and heated 25 – 350 °C with heating rate of 10 °C/min under nitrogen flow 50 ml/min. Measurements were performed on DSC 1 (Mettler-Toledo AG, Analytical, Switzerland), and results were normalized to sample weight and evaluated by STAR® SW 12.10 software.

2.7.3.　X-ray powder diffraction analysis (XRPD)—Measurements were conducted on Rigaku Smartlab X-ray Diffractometer in θ-θ geometry (the sample in horizontal position) in parafocusing Bragg-Brentano geometry using D/teX Ultra 250 strip detector in 1D standard mode with CuKα1,2 radiation source (U = 40 kV and I = 30 mA). The XRPD patterns were collected in 3–40° 2θ range, with step of 0.01°, and data collection speed of 3 °/min. The low background single crystal silicon sample holder was used to minimize the background.

2.8. Dissolution study

Dissolution studies were performed by reverse dialysis bag method with 6 time points sampling (5 min, 15 min, 30 min, 1 h, 2 h and 3 h). Mixture of water (pH 5.5) and isopropanol 90:10 (v/v) was used as dissolution medium. Dialysis bags (cellulose membrane, MW cut-off 12000, Sigma Aldrich Chemie GmbH, Germany) filled with 5 ml of dissolution medium were immersed in 200 ml of the same medium in which 2 ml of the nanosuspension formulation (NS2, NS4, NS5 or NS6) or suspension (S2, S4, S5 or S6) was added. For the dissolution of pure DK-I-56–1, 4 mg of substance powder was added. Experiments were performed at 37 ± 2 °C under constant stirring (ES-20 orbital shaker-incubator, Biosan SIA, Latvia). The dialysis bag content was sampled in appropriate intervals and analyzed by LC-MS/MS. Measurements were done in triplicates.

For formulation comparison, univariate ANOVA was applied, with $P<0.05$ considered as statistically significant.

2.9. In vivo pharmacokinetic and biodistribution studies

2.9.1. Formulations for pharmacokinetic and biodistribution studies—For *in vivo* studies, nanosuspension (NS2-P), solution (SOL) and suspension (SUSP) with 2 mg/ml DK-I-56–1 were used. Tonicity of NS2-G, nanosuspension stabilized by polysorbate 80, was adjusted by 2.5% glycerol and checked by osmometer (Osmometer Model 3320, Advanced Instruments, Inc., SAD, Advanced®). This formulation was characterized in terms of particle size and polydispersity index. Solution (SOL) with the same concentration of DK-I-56–1 was prepared by dissolving the ligand in mixture of 20% dimethyl-sulfoxide, 20% Cremophor EL and 60% saline (Fan et al., 2018). For the suspension (SUSP) formulation, DK-I-56–1 was mixed with vehicle containing 1% polysorbate 80, 14% propylene glycol, and 85% water, and vortexed for several minutes (Knutson et al., 2018).

2.9.2. Animals and dosing—Male C57BL/6 mice weighing 23–33 g were housed three to four animals per cage, on a 12 h light/dark period (light on at 6:00 a.m). The temperature in the animal room was maintained at 22 ± 1 °C, with the relative humidity 40%–70%, and the illumination 120 lx. The pelleted food and tap water were provided *ad libitum* throughout the experiment. The study was conducted according to the National Institutes of Health Animal Care and Use Committee guidelines, and was approved by the Ethical Committee on Animal Experimentation of the University of Belgrade – Faculty of Pharmacy, Serbia. Experimental animals were divided in three groups – NS2-G, SOL and SUSP, each containing 18 animals (for each formulation, three animals were used per time point). All formulations were administered i.p. in a volume of 2 ml/kg to obtain a dose of 10 mg/kg. The treatments were well tolerated, without signs of local irritation.

2.9.3. Plasma and tissue sampling processing—At predetermined time intervals (5 min, 20 min, 1 h, 4 h, 16 h and 36 h) animals were anesthetized by ketamine hydrochloride (90 mg/kg, 10% Ketamidor, Richter Pharma AG, Wels, Austria), and samples of blood (collected via cardiac puncture in heparinized syringes), liver, kidney and brain were taken. Plasma was obtained after centrifugation for 10 min at $1000 \times g$ (MiniSpin® plus centrifuge, Eppendorf, Germany). Tissue samples were weighted and homogenized in 1.25 ml (liver and brain) or 1 ml (kidney) of methanol via ultrasonic probe (70% amplitude 2 $\times$ 20 s for brain, 80% amplitude 3 $\times$ 20 s for liver and kidney). Supernatants were separated after centrifugation for 20 min at $3400 \times g$ (MiniSpin® plus centrifuge, Eppendorf, Germany). The obtained plasma and supernatants were further processed with solid phase extraction (Oasis HLB cartridges, Waters Corporation, Milford, Massachusetts). Cartridges were preconditioned with methanol and water, loaded with samples and the internal standard solution, and DK-I-56–1 was eluted by 1 ml of methanol for 1 min. DK-I-56–1 concentration in obtained eluates was analyzed by LC-MS/MS. Pharmacokinetic parameters were calculated using "PK Functions for Microsoft Excel" (https://www.pharmpk.com/soft.html) and expressed as mean ± S.E.M. Statistical analysis was done using IBM SPSS Statistics software (v.25); for results with normal distribution, one-way ANOVA with Turkey

HSD as post hoc was used, while for results without normal distribution, Kruskal-Wallis test was used. In both cases, $P < 0.05$ was considered as statistically significant.

2.10. In vivo pharmacodynamic study

Spontaneous locomotor activity (SLA) assay was carried out on experimentally naïve 9–11 weeks old male C57BL/6 mice weighing 20–26 g. The behavior was analyzed by ANY–maze Video Tracking System (Stoelting Co, Wood Dale, IL, USA). NS2-G, placebo (PLA) or saline (SAL) formulations were administered i.p. in a volume of 5 ml/kg to obtain a dose of 10 mg/kg. Activity of single rats in a clear Plexiglas chamber ($40 \times 25 \times 35$ cm) under dim red light (20 lx) was recorded for a total of 90 min, without any acclimatization period (Knutson et al., 2018). The parameters analyzed were total distance travelled (m) and total time immobile (s). Immobility sensitivity was set to 65% (percentage of the animal which has to remain in the same place for the animal to be considered immobile). All data are expressed as mean ± S.E.M. The parameters were assessed by a one-way ANOVA, with treatment as between subject factor, with exception of the 15-min bins data, subjected to two-way repeated measures ANOVA (SigmaPlot 12.0, Chicago, USA). Post hoc comparisons, where applicable, were performed using SNK test.

2.11. Analytical methods

Concentration of DK-I-56–1 was determined using liquid chromatography – tandem mass spectrometry (LC-MS/MS) method. The analysis was performed on UHPLC chromatograph ACELLA (Thermo Fisher Scientific Inc., Madison, WI, USA), coupled to a triple quadrupole mass spectrometer TSQ Quantum Access MAX (Thermo Fisher Scientific Inc., Madison, WI, USA) with heated electrospray ionization (HESI) interface. The column was XTerra MS C18 (150 mm x 2.1 mm, 3.5 µm particle size). Mobile phase was acetonitrile/ 0.1% formic acid = 50:50 (v/v), flow rate was 0.3 ml/min, column temperature was set to 35 ℃ and injection volume was 10 µl. DK-I-56–1 and internal standard (for *in vivo* studies) were detected and quantified in positive HESI mode (m/z = 325.3–307.2 and m/z = 327.8–320.9, respectively).

3. Results and discussion

3.1. Solubility study

Deuterated pyrazoloquinolinone ligand, DK-I-56–1 (Figure 1), with logP 2.06 and molecular weight 325.14, was investigated as a lead compound for various neuropsychiatric disorders (Knutson et al., 2018). The coarse powder of DK-I-56–1 was yellow, with particles varying in shape and size (D(v, 0.1) 17.2 ± 2.1 µm, D(v, 0.5) 130.0 ± 61.6 µm and D(v, 0.9) 757.0 ± 389.0 µm). The solubility study showed that DK-I-56–1 is practically insoluble in investigated solvents, except in DMSO (Table 1). Although in preclinical studies DMSO can be used for parenteral administration in concentrations up to 20%, safety issues for a DMSO-based formulation would still be a serious concern (Williams et al., 2013), having in mind its low maximum allowable limit established by FDA (1998). Among several insoluble drug delivery strategies (Kalepu and Nekkanti, 2015), nanonization seemed to be most appropriate to physicochemical properties of DK-I-56–1, such as poor solubility in water,

high molecular weight and high melting point of 312.52 °C (cf. Van Eerdenbrugh et al., 2008).

The solubility of DK-I-56–1 was examined in solutions of the stabilizers in the same concentration as that used in nanosuspensions (Table S1). As expected, stabilizers that were used in concentrations below their critical micelle concentration (CMC) – poloxamer 188 and poloxamer 407 (Kabanov et al., 2002; Deng et al., 2010), did not alter DK-I-56–1 solubility in water. On the other hand, TPGS and polysorbate 80 enhanced DK-I-56–1 solubility due to phenomena of micellar solubilization (Zhang et al., 2012), while the solubility in different polysorbate 80 dispersions was enhanced as the surfactant concentration increased.

3.2. Physicochemical characterization and stability study

3.2.1. Particle size analysis, zeta potential measurements and stability study

—Nanosuspensions of DK-I-56–1 stabilized by different steric stabilizers and their combinations were prepared by small scale media milling technique similar to protocol explained by Corrias et al. (2017). Parenteral route of administration limits number of stabilizers that can be used, so typical non-ionic stabilizers such as polysorbate 80 and poloxamers were chosen. Although TPGS has not been approved for parenteral administration yet, their frequent uses as a stabilizer in nanosuspensions and growing interest for exploring its use in this route of administration (Ahire et al., 2018) were the reasons for investigating its stabilizing potential in this research. In formulations stabilized by polysorbate 80 alone (NS1, NS2 and NS3), stabilizer concentration increase led to initial nanocrystal size decrease (Figure 2), which was an expected finding (Van Eerdenbrugh et al., 2009). However, one day after preparation, an extensive agglomeration occurred in NS1 and NS3 formulations, while z-ave remained around 200 nm in NS2 (Figure 2). Drug particles interact with stabilizer molecules during milling, which results in their adsorption on particle surface. It is advisable to use stabilizers in concentrations bellow their critical micelle concentration (CMC), in order to avoid micelles formation. In concentrations well above CMC, micelles begin to compete for particle surface adsorption, so the total surfactant coverage begins to decrease (Deng et al., 2010). This could be the reason for instabilities observed in formulation NS3. Thereby, NS1 and NS3 were excluded from further experiments.

Further formulation studies investigated efficacy of other surfactant agents in combination with polysorbate 80. As mentioned above, poloxamer 188 and poloxamer 407 were used in concentrations bellow CMC at 25 °C while TPGS was used in concentration above CMC. DLS results suggest that these steric stabilizers readily adsorb on particle surface, and thus enhance stability of nanocrystal particles. Addition of another steric stabilizer in NS1 formulation contributed to better stabilization of nanocrystals, which resulted in particle size preservation over time (Figure 2). Laser diffraction measurements confirmed submicron size of nanosuspensions NS2, NS4, NS5 and NS6, with D(v, 0.9) well below 1 μm (Table S2), making these formulations safe for parenteral administration (Wang et al., 2017). Mean hydrodynamic diameter of selected formulations changed slightly over this period, without significant changes in PDI (F(1,4) = 0.604, P = 0.480) (Figure 2). With narrow

particle size distribution, solubility differences of particles with different size were kept at minimum, which alongside with poor solubility in water of DK-I-56–1 prevented Ostwald ripening (Wang et al., 2013). However, particle growth over time is inevitable problem of nanosuspensions, so their stability was usually restricted to short periods of two weeks (Sharma et al., 2011), one month (Pardeike et al., 2010) or six weeks at 25 °C (Dolenc et al., 2009). As additional stability indicator, zeta potential of selected nanosuspensions was measured (Table S2). The values around −20 mV are considered as markers of good stability for nanosuspensions stabilized by non-ionic stabilizers. As mere zeta potential is insufficient for stability evaluation (Bhattacharjee, 2016), its combined analysis with particle sizing indicated that selected nanosuspensions show good short term stability, adequate for formulations intended for preclinical studies (Merisko-Liversidge and Liversidge, 2011).

3.2.2.   Atomic force microscopy (AFM)—For non-spherical particles, DLS provide hydrodynamic radius of a hypothetical hard sphere moving at the same speed as aspherical nanoparticle in dispersion (Bhattacharjee, 2016), which is important for the interpretation of results. For example, in case of nanorods, two peaks on DLS intensity diagram could be attributed to longitudinal and transverse size, respectively (Pan et al., 2007). In case of such particles, microscopic analysis for particle sizing could be beneficial. As AFM provides precise information on particle size and shape with high nano-range resolution, it was applied in order to get more insight into particle morphology. Clear visualization of single nanocrystal particle in undiluted sample was difficult, probably due to aggregation during sample preparation (Figure S1). On the other side, single particles as well as aggregates formed during water evaporation could be observed in AFM images taken from diluted NS2 sample (Figure 3a, 3b and 3d). The particle marked on Figure 3c with ellipsoid shape had dimensions of around 190 nm (width), 400 nm (length) and 35 nm (height) (Figure 3e). When comparing to z-ave 249.6 ± 3.4 nm, particle size shifting could be attributed to their non-spherical shape. Considering that low resolution of DLS hinders distinguishing longitudinal and transverse size in this case, it could be concluded that the obtained results from AFM were in good agreement with DLS measurements.

3.2.3.   Physical state evaluation—Wet ball milling as a high energy process could produce disorders or cleavage of crystal lattice of the drug substance at the weakest sites, or even induce amorphisation (Steckel et al., 2003; Wang et al., 2017). Maintaining drug crystallinity in nanosuspensions is beneficial for their stability, because differences in solubility can induce crystal growth in systems containing mixture of amorphous and crystal form (Chin et al., 2014; Wang et al., 2013). Therefore, existence of possible crystal lattice defects, polymorphic transition and/or amorphisation of the drug in nanosuspensions must be assessed. As it could be concluded from DSC studies (Figure 4), DK-I-56–1 has a high melting point at 312.52 °C. On DSC curves of samples prepared from suspension and nanosuspension, a sharp melting peak at temperatures from 311.38 to 312.80 °C was visible (Figure 4). Because of defects in crystal lattice formed during formulation preparation, the melting point of a drug could be shifted (Yang et al., 2014). However, the observed minimal differences in peak temperatures could be explained by normal variability in measurement, and should not be seen as a sign of change of polymorphic form of DK-I-56-1.

Powder X-ray diffraction measurements were performed in order to deepen the analysis of physical state of DK-I-56–1 in formulations. Higher baseline in XRPD patterns from nanocrystal samples was probably caused by existence of amorphous layer of polysorbate 80 on dried samples (Ali et al., 2011). Sharp peaks at 2-theta 4.73; 5.46; 9.87; 16.95 and 17.66° visible on diffractogram of DK-I-56–1, were present on PRXD patterns of suspension and nanosuspension samples (Figure 5). These peaks can be used as a confirmation of retained crystal structure of DK-I-56–1 in investigated samples. Broadening of the peaks in nanosuspension samples compared to physical mixture (suspension) and coarse drug samples can be characterized as a consequence of particle size reduction, i.e. existence of nanocrystalline phase (Bates et al., 2006). Interestingly, two close peaks in diffractogram of unprocessed drug at 2-theta 6.09 and 6.38° (Figure 5a) cannot be observed in nanocrystal samples. The disappearance of the mentioned peaks could be explained by dilution effect (Huang et al., 2013), together with effect of particle size reduction (Bates et al., 2006), This statement could be supported by XRPD pattern of physical mixture (S2), where only a broad peak with very small intensity can be detected at 6.38° (Figure 5b). It was possible that diffraction line broadens further due to nanonization, and eventually sinks below baseline. Difficulties in analyzing results from XRPD measurements arise from lack of the literature data on the crystal form of DK-I-56–1 or possible polymorphism. However, results from DSC and XRPD measurements undoubtedly confirmed that DK-I-56–1 remained in crystal state after nanonization.

3.3. Dissolution studies

Particle size reduction changes dissolution rate of the drug, according to Noyes-Whitney equation (Dolenc et al., 2009; Yang et al., 2014). However, a major obstacle for dissolution studies of nanosuspensions is separation of undissolved particles from the dissolved drug (Chen et al., 2017). Therefore, using dialysis bag method as a separation technique could be advantageous. Dissolution profiles of pure DK-I-56–1, nanosuspensions (NS2, NS4, NS5 and NS6) and corresponding physical mixtures (S2, S4, S5 and S6) are shown in Figure S2. Dissolution of DK-I-56–1 in physical mixtures was only slightly influenced by excipients when compared to the dissolution of DK-I-56–1 alone. Similar findings could be found for aripiprazole (Xu et al., 2012), herpetrione (Guo et al., 2013), fenofibrate (Yang et al., 2014) and ritonavir (Karakucuk et al., 2019). On the other hand, nanonization increased the dissolution rate in NS2, NS5 and NS6 (Figure S2a, S2c and S2d), but not NS4 when compared to physical mixture. It is possible that nanocrystals in NS4 aggregated upon dilution at 37 °C, which resulted in similar dissolution profiles of nanosuspension and corresponding suspension (Figure S2b). Indeed, Deng et al. observed in one of the formulations of paclitaxel nanocrystals (stabilized by poloxamer 407) that particle size increased after dilution and incubation at 37 °C. They explained their finding by inhibition of surfactant adsorption on nanocrystal surface at higher temperatures, making the crystals prone to aggregate (Deng et al., 2010). Of all investigated nanosuspensions, the nanonization influence on dissolution rate was the most pronounced in case of NS2. However, despite a significant twofold increase of dissolution rate of nanosuspension NS2, it was still limited by very poor solubility (Ganta et al., 2009; Yang et al., 2014), with around 63% of DK-I56–1 dissolved in 3 h. Nevertheless, the observed dissolution rate differences could be undoubtedly associated with smaller particle size.

3.4. In vivo pharmacokinetic and biodistribution studies

Pharmacokinetic study was performed in order to evaluate *in vivo* fate of nanosuspension after i.p. administration in mice mice at a well-tolerated dose (Knutson et al., 2018, Vasovi et al., 2018), and investigate its suitability for preclinical pharmacokinetic studies. In line with general recommendation for parenteral preparations to keep qualitative and quantitative composition as simple as possible, nanosuspension stabilized by polysorbate 80 alone was chosen for *in vivo* experiments, with addition of glycerol as tonicity adjuster. After preparation, nanosuspension formulation (NS2-G) was with z-ave of 273.3 ± 2.2 nm and PDI of 0.263 ± 0.017. Formulation was considered as suitable for parenteral administration with low polysorbate 80 concentration, small particle size and osmolality 289 mOsm/kg. SOL formulation was yellow, with no separation of phases, while SUSP formulation was easily re-dispersed into homogenous suspension by manual shaking and applying ultrasound before administration (Figure S3). However, particle size distribution of suspension was broad, with D(v, 0.1) 1.40 ± 0.01 μm, D(v, 0.5) 12.97 ± 0.58 μm and D(v, 0.9) 87.33 ± 2.63 μm.

Three formulations of DK-I-56–1 (NS2-G, SOL and SUSP) were administered i.p. and their pharmacokinetic profiles as well as biodistribution of DK-I-56–1 were analyzed. Generally, clearance of the drugs from the peritoneal cavity is driven by the diffusion into surrounding tissues, after which the drug is carried away by capillary blood or lymph, metabolized by tissue enzymes or bound to tissue proteins, resulting in relatively fast drug absorption (Claassen, 1994). Area under the curve values (AUC_{0-36}), reflecting availability calculated from plasma concentration-time curves, were significantly different for three formulations ($F(2,6) = 39.280$, $P < 0.001$). After administration, highest plasma concentrations of DK-I-56–1 were achieved after SOL, which was followed by NS2-G and SUSP, respectively, and the same trend was observed for plasma AUC_{0-36} values (Figure 6a). Probably, Cremophor EL and DMSO increased the absorption rate, thus enabling higher plasma levels after SOL administration (Buggins et al., 2007). Considering high quantities of excipients used in SOL formulation (molar ratio of DK-I-56–1/DMSO/Cremophor EL was 1/413/236), it could be assumed that they can have an impact on DK-I-56–1 distribution as well. Cremophor EL is widely used solubilizer in parenteral formulations for numerous poorly soluble drugs, but it may exert a range of biological effects, including changes in drug disposition (Gelderblom et al., 2001). It was stated that Cremophor EL, by changing drug-protein interactions, influences paclitaxel and doxorubicin distribution (Badary et al., 1998; Sykes et al., 1994). This could be an important factor in DK-I-56–1 pharmacokinetics as well, because its free fraction was reported to be low (0.194) (Knutson et al., 2018). Brain availability after SOL administration was not higher than after NS2-G and SUSP ($H(2) = 0.622$, $P = 0.733$), despite superior plasma levels (Figure 6b). In high concentrations, DMSO can act as a blood brain barrier opener, allowing higher drug passage to the brain, although literature data is not consistent in this matter (Buggins et al., 2007). However, in this research only $3.12 \pm 0.38\%$ of total AUC_{0-36} (sum of AUC_{0-36} in four investigated compartments) reached the brain after SOL, and this brain portion of DK-I-56–1 was similar as in case of other two formulations ($3.79 \pm 1.48\%$ and $3.48 \pm 2.21\%$, for NS2-G and SUSP, respectively), indicating absence of the suggested effect of DMSO. Additionally, according to elimination half-life, DK-I-56–1 retained in brain for a longer time when

administered as nanosuspension, compared to solution (Figure 6b). AUC_{0-36} values in liver and kidney were not significantly different ($F(2,6) = 0.332$, $P = 0.730$ and $H(2) = 0.356$, $P = 0.837$, respectively) between three formulations, and concentration profiles after NS2-G and SOL were similar (Figure 6c and Figure 6d). Actually, higher percentage of total AUC_{0-36} remained in blood after SOL ($19.52 \pm 1.11\%$, compared to $11.83 \pm 4.75\%$ and $1.43 \pm 0.48\%$ after NS2-G and SUSP, respectively), while the calculated tissue percentages were similar for all three formulations (around 3% in brain, 40% in liver and 50% in kidney). This confirms a suggestion that influence of Cremophor EL on distribution may be profound only in central blood compartment (Gelderblom et al., 2001). Interestingly, total AUC_{0-36} in plasma and organs after SOL was substantially lower than after NS2-G and SUSP (52368.97 ± 4502.09; 75459.86 ± 26699.73 and 86880.56 ± 29533.80 ng·h/ml, respectively), indicating that SOL formulation gave rise to an enhanced elimination from the body. Some reports state nephrotoxicity of DMSO and Cremophor EL, with tubular cells necrosis and oliguria Pestel et al., 2006; Buggins et al., 2007), which could contribute to non-physiological handling of DK-I-56–1 from SOL. Therefore, a simplistic formulation of NS2-G, without any organic solvent and with low surfactant concentration, may be thought of as a major advantage over SOL formulation, through obviating erratic pharmacokinetic behavior and toxicity caused by excipients.

A smaller particle size of nanosuspension, and therefore an increased surface area available for dissolution, was the most probable reason for faster absorption and higher systemic exposure of DK-I-56–1 after nanosuspension when compared to suspension administration. This was supported by results from *in vitro* dissolution studies (Figure S2). Similarly, in the research of Sigfridsson et al. AUC and C_{max} of the novel substances AC88 and BA99 were about twice as high for the animals receiving nanosuspensions compared to the ones receiving microsuspensions via intraperitoneal administration (Sigfridsson et al., 2013). On the other hand, brain AUC_{0-36} after NS2-G and SUSP were similar ($P = 0.733$). However, concentration profile in brain after SUSP administration showed bimodal distribution with the concentration drop after 1h (Figure 6b), and the same behavior of this formulation could be noticed in liver and kidney as well (Figure 6c and Figure 6d). The explanation of this phenomenon could be found in formation of DK-I-56–1 depot at the site of administration due to small quantities of liquid available for dissolution, resulting in erratic absorption and distribution, as observed in case of intramuscular and subcutaneous injections (Zuidema et al., 1994). Because of bimodal distribution, and despite high tissue AUC values, DK-I-56–1 concentration in brain after suspension administration was smaller than after other two treatments in most time points, which could compromise its efficacy. Main advantage of NS2-G over SUSP would therefore be a smaller drug particle size and narrower particle size distribution, leading to a reliable bioavailability and more regular pharmacokinetics, which is important in preclinical studies of drug candidates with poor solubility.

3.5. In vivo pharmacodynamic study

Studies of motor activity can explain the effect of the administered drug substance on experimental animals' behavior, and they represent one of the fundamental approaches during investigation of psychopharmacological drugs (Savi et al., 2006). Spontaneous locomotor activity (SLA) test is one of behavioral tests used by our group for examining

drugs' activity on $GABA_A$ receptors (Savi et al., 2010; Savi et al., 2008). The term 'spontaneous locomotor activity' is referred to a group of unconditioned tests in which parameters of motion are followed. Based on their influence on locomotor activity in rodents, many psychotropic substances are defined as stimulant or depressant (Geyer, 1990). Hyperlocomotion after DK-I-56–1 administration in rats was already reported by Knutson et al. (2018). Specific mechanism of this action has not been fully explained yet, which requires further efforts to identify the underlying biological substrate. However, nanoemulsion used as the carrier of DK-I-56–1 in the cited research also exhibited a mild behavioral activity, possibly due to its complex composition, which complicated interpretation of results. Therefore, SLA analysis was performed in order to assess use of nanosuspensions in pharmacodynamic characterization of DK-I-56–1, especially regarding potential influence of delivery system on the obtained results. Statistical analysis showed a significant effect of NS2-G treatment on total distance travelled during 90 min of monitoring ($F_{(2,29)} = 7.126$, $P = 0.003$). As shown on Figure 7a, the hyperlocomotor effect of DK-I-56–1 in NS2-G was significant compared to placebo, as well as to saline control, while no significant differences were noticed between placebo and saline ($P = 0.289$). These findings proved that observed hyperlocomotion effect was a consequence of DK-I-56–1 activity only, without any contribution of the used vehicle. Combined electrophysiological and pharmacokinetic results presented in Knutson et al. (2018) suggest that the free (unbound) brain concentration of DK-I-56–1 in the range close to 100 nM is sufficiently high to mediate the pharmacological effect. Hence, the performed spontaneous locomotor activity test in mice confirmed results from pharmacokinetic studies of delivering effective concentration of DK-I-56–1 to the brain by i.p. administered nanosuspension as advanced formulation technique. Present results also showed that hyperlocomotor effect of DK-I-56–1 was more profound during the last 45 min of experiment ($F_{(2,145)} = 7.126$, $P = 0.003$; $F_{(5,145)} = 92.474$, $P < 0.001$, vs. PLA and SAL, respectively) (Figure 7b), suggesting that it was not predominantly based on influences on habituation/stress reaction to novelty. When animals are exposed to the new environment, they exhibit curiosity and fear, which act as exploratory drive. However, after habituation, this exploratory drive decreases, and the emitted behavior may rather reflect a general, spontaneous locomotor activity (Savi et al., 2006). This was particularly evident for the total time immobile (Figure S4a) which is recognized as a more robust parameter than total distance travelled. This parameter is of specific interest in cases when animal stops changing its location, but continuous to move parts of its body (example: head motions). Total time immobile was affected in the same manner as total distance travelled ($F_{(2,29)} = 11.887$, $p < 0.001$), and differences between NS2-G and other two treatments were more pronounced in the second half of the experiment ($F_{(2,145)} = 11.885$, $P < 0.001$; $F_{(5,145)} = 74.265$, $P < 0.001$; $F_{(10,145)} = 2.938$, $P = 0.002$, vs. PLA, SAL and interaction time x treatment, respectively; Figure S4b). Hence, preservation of hyperlocomotion, that was observed after habituation in animals treated with NS2-G, represented a clear evidence of the DK-I-56–1 action solely.

4. Conclusion

Four formulations of nanosuspensions of DK-I-56–1 with desirable physicochemical characteristics and short-term stability appropriate for formulations for preclinical studies

were developed. Their small particle size and narrow size distribution made them suitable for parenteral administration. Crystalline state of DK-I-56–1 was not affected by preparation method, which excludes potential stability issues regarding its solid state. Pharmacokinetic study emphasized advantages of nanosuspension over solution and suspension. Low surfactant concentration and absence of organic solvents reduced the risk of potential influence of excipients on DK-I-56–1 pharmacokinetics, and small particle size led to an optimized balance of brain-to-plasma bioavailability after nanosuspension administration. Moreover, behavioral study confirmed that nanosuspensions could deliver DK-I-56–1 to brain in pharmacologically effective concentration. Based on the lack of behavioral activity of placebo formulation, nanosuspension might serve as an applicable delivery strategy for pharmacodynamic investigation of poorly water-soluble substances of the pyrazoloquinolinone chemotype, such as DK-I-56–1.

Supplementary Material

Refer to Web version on PubMed Central for supplementary material.

Acknowledgment

References

Ahire E, Thakkar S, Darshanwad M, Misra M, 2018. Parenteral nanosuspensions: a brief review from solubility enhancement to more novel and specific applications. Acta Pharm. Sin. B 8(5), 733–755. doi: 10.1016/j.apsb.2018.07.011 [PubMed: 30245962]

Ali HS, York P, Ali AM, Blagden N, 2011. Hydrocortisone nanosuspensions for ophthalmic delivery: a comparative study between microfluidic nanoprecipitation and wet milling. J. Control. Release 149(2), 175–181. doi: 10.1016/j.jconrel.2010.10.007 [PubMed: 20946923]

Ayad MH, 2015. Rational formulation strategy from drug discovery profiling to human proof of concept. Drug Deliv. 22(6), 877–884. doi: 10.3109/10717544.2014.898714 [PubMed: 24670097]

Badary OA, Al-Shabanah OA, Al-Gharably NM, Elmazar MM, 1998. Effect of Cremophor EL on the Pharmacokinetics, Antitumor Activity and Toxicity of Doxorubicin in Mice. Anticancer Drugs 9(9), 809–815. doi: 10.1097/00001813-199810000-00011 [PubMed: 9840728]

Bates S, Zografi G, Engers D, Morris K, Crowley K, Newman A, 2006. Analysis of amorphous and nanocrystalline solids from their X-ray diffraction patterns. Pharm. Res 23(10), 2333–2349. doi: 10.1007/s11095-006-9086-2 [PubMed: 17021963]

Bhattacharjee S, 2016. DLS and zeta potential - What they are and what they are not? J. Control. Release 235, 337–351. doi: 10.1016/j.jconrel.2016.06.017 [PubMed: 27297779]

Buggins TR, Dickinson PA, Taylor G, 2007. The effects of pharmaceutical excipients on drug disposition. Adv. Drug Deliv. Rev 59(15), 1482–1503. doi: 10.1016/j.addr.2007.08.017 [PubMed: 18198495]

Chen ML, John M, Lee SL, Tyner KM, 2017. Development Considerations for Nanocrystal Drug Products. AAPS J 19(3), 642–651. doi: 10.1208/s12248-017-0064-x [PubMed: 28281194]

Chin WW, Parmentier J, Widzinski M, Tan EH; Gokhale R, 2014. A brief literature and patent review of nanosuspensions to a final drug product. J. Pharm. Sci 103(10), 2980–2999. doi: 10.1002/jps.24098 [PubMed: 25099918]

Chiou LC, Cook J, Ernst M, Fan PC, Knutson D, Meirelles M, Mihovilovic M, Sieghart W, Varagic Z, Verma R, Wimmer L, Witzigmann C, Siebert DCB, Savic MM, 2018a. Ligands selective to alpha 6 subunit-containing GABAAa receptors and their methods of use. U. S. Patent Application No. 15/578,790.

Chiou LC, Lee HJ, Ernst M, Huang WJ, Chou JF, Chen HL, Mouri A, Chen LC, Treven M, Mamiya T, et al. , 2018b. Cerebellar α6 -subunit-containing GABAA receptors: a novel therapeutic target for disrupted prepulse inhibition in neuropsychiatric disorders. Br. J. Pharmacol 175(12), 2414–2427. doi: 10.1111/bph.14198 [PubMed: 29518821]

Claassen V, 1994. Intraperitoneal drug administration. Neglected Factors in Pharmacology and Neuroscience Research. Techniques in the Behavioral and Neural Sciences, 12. doi: 10.1016/B978-0-444-81871-3.50010-2

Corrias F, Schlich M, Sinico C, Pireddu R, Valenti D, Fadda AM, Marceddu S, Lai F, 2017. Nile red nanosuspensions as investigative model to study the follicular targeting of drug nanocrystals. Int. J. Pharm 524(1–2), 1–8. doi: 10.1016/j.ijpharm.2017.03.042 [PubMed: 28336458]

Deng J, Huang L, Liu F, 2010. Understanding the Structure and Stability of Paclitaxel Nanocrystals. Int. J. Pharm 390(2), 242–249. doi: 10.1016/j.ijpharm.2010.02.013 [PubMed: 20167270]

Dolenc A, Kristl J, Baumgartner S, Planinšek O, 2009. Advantages of celecoxib nanosuspension formulation and transformation into tablets. Int. J. Pharm 376, 204–212. doi: 10.1016/j.ijpharm.2009.04.038 [PubMed: 19426794]

Fan PC, Lai TH, Hor CC, Lee MT, Huang P, Sieghart W, Ernst M, Knutson DE, Cook J, Chiou LC, 2018. The α6 subunit-containing GABA A receptor: A novel drug target for inhibition of trigeminal activation. Neuropharmacology 140, 1–13. doi: 10.1016/j.neuropharm.2018.07.017 [PubMed: 30016665]

FDA, Guidances, Appendix 6. Toxicological Data For Class 3 Solvents. U. S. Food & Drug Administration, 1998. (available at www.fda.gov/downloads/drugs/guidancecomplianceregulatoryinformation/guidances/ucm07340 3.pdf (Accessed 1/29/2020).

Frank KJ, Boeck G, 2016. Development of a nanosuspension for iv administration: From miniscale screening to a freeze dried formulation. Eur. J. Pharm. Sci 87, 112–117. doi: 10.1016/j.ejps.2016.03.003 [PubMed: 26970283]

Ganta S, Paxton JW, Baguley BC, Garg S, 2009. Formulation and pharmacokinetic evaluation of an asulacrine nanocrystalline suspension for intravenous delivery. Int. J. Pharm 367(1–2), 179–186. doi: 10.1016/j.ijpharm.2008.09.022 [PubMed: 18848873]

Gao Y, Li Z, Sun M, Li H, Guo C, Cui J, Li A, Cao F, Xi Y, Lou H, et al. , 2010. Preparation, characterization, pharmacokinetics, and tissue distribution of curcumin nanosuspension with TPGS as stabilizer. Drug Dev. Ind. Pharm 36(10), 1225–1234. doi: 10.3109/03639041003695139 [PubMed: 20545506]

Gelderblom H, Verweij J, Nooter K, Sparreboom A, 2001. Cremophor EL: The Drawbacks and Advantages of Vehicle Selection for Drug Formulation. Eur. J. Cancer 37(13), 1590–1598. doi: 10.1016/s0959-8049(01)00171-x [PubMed: 11527683]

George M, Ghosh I, 2013. Identifying the correlation between drug/stabilizer properties and critical quality attributes (CQAs) of nanosuspension formulation prepared by wet media milling technology. Eur. J. Pharm. Sci 48(1–2), 142–152. doi: 10.1016/j.ejps.2012.10.004 [PubMed: 23085547]

Geyer MA Approaches to the characterization of drug effects on locomotor activity in rodents. In: Adler MW, and Cowan A. editors. Modern Methods in Pharmacology Vol. 6 Testing and Evaluation of Drug Abuse, Wiley Liss; 1990. p. 81–100.

Grohganz H, Priemel PA, Löbmann K, Nielsen LH, Laitinen R, Mullertz A, Van den Mooter G, Rades T, 2014. Refining stability and dissolution rate of amorphous drug formulations. Expert. Opin. Drug Deliv 11(6), 977–989. doi: 10.1517/17425247.2014.911728 [PubMed: 24754747]

Guo JJ, Yue PF, Lv JL, Han J, Fu SS, Jin SX, Jin SY, Yuan HL, 2013. Development and in vivo/in vitro evaluation of novel herpetrione nanosuspension. Int. J. Pharm 441(1–2), 227–233. doi: 10.1016/j.ijpharm.2012.11.039 [PubMed: 23220096]

Huang Y, Luo X, You X, Xia Y, Song X, Yu L, 2013. The preparation and evaluation of water-soluble SKLB610 nanosuspensions with improved bioavailability. AAPS Pharm. Sci. Tech 14(3), 1236–1243. doi: 10.1208/s12249-013-0005-7

Kabanov AV, Batrakova EV, Alakhov VY, 2002. Pluronic block copolymers as novel polymer therapeutics for drug and gene delivery. J. Control. Release 82(2–3), 189–212. doi: 10.1016/s0168-3659(02)00009-3 [PubMed: 12175737]

Kalepu S, Nekkanti V, 2015. Insoluble drug delivery strategies: review of recent advances and business prospects. Acta Pharm. Sin. B 5(5), 442–453. doi: 10.1016/j.apsb.2015.07.003 [PubMed: 26579474]

Karakucuk A, Teksin ZS, Eroglu H, Celebi N, 2019. Evaluation of improved oral bioavailability of ritonavir nanosuspension. Eur. J. Pharm. Sci 131, 153–158. Doi: 10.1016/j.ejps.2019.02.028

Knutson DE, Kodali R, Divovi B, Treven M, Stephen MR, Zahn NM, Dobri i V, Huber AT, Meirelles MA, Verma RS, et al. , 2018. M. Design and Synthesis of Novel Deuterated Ligands Functionally Selective for the γ-Aminobutyric Acid Type A Receptor (GABAAR) α6 Subtype with Improved Metabolic Stability and Enhanced Bioavailability. J. Med. Chem 61(6), 2422–2446. doi: 10.1021/acs.jmedchem.7b01664 [PubMed: 29481759]

Liu T, Müller RH, Möschwitzer JP, 2015. Effect of drug physico-chemical properties on the efficiency of top-down process and characterization of nanosuspension. Expert. Opin. Drug Deliv 12(11), 1741–1754. doi: 10.1517/17425247.2015.1057566 [PubMed: 26098043]

Merisko-Liversidge E, Liversidge GG, 2011. Nanosizing for Oral and Parenteral Drug Delivery: A Perspective on Formulating Poorly-Water Soluble Compounds Using Wet Media Milling Technology. Adv. Drug Deliv. Rev 63(6), 427–440. doi: 10.1016/j.addr.2010.12.007 [PubMed: 21223990]

Müller RH, Gohla S, Keck CM, 2011. State of the art of nanocrystals--special features, production, nanotoxicology aspects and intracellular delivery. Eur. J. Pharm. Biopharm 78(1), 1–9. doi: 10.1016/j.ejpb.2011.01.007 [PubMed: 21266197]

Müller RH, Jacobs C, Kayser O, 2001. Nanosuspensions as particulate drug formulations in therapy Rationale for development and what we can expect for the future. Adv. Drug Deliv. Rev 47(1), 3–19. doi: 10.1016/s0169-409x(00)00118-6 [PubMed: 11251242]

Pan B, Cui D, Xu P, Li Q, Huang T, He R, Gao F, 2007. Study on interaction between gold nanorod and bovine serum albumin. Coll. Surf. A: Physicochem. Eng. Aspects 295(1-3), 217–222. doi: 10.1016/j.colsurfa.2006.09.002

Pardeike J, Müller RH, 2010. Nanosuspensions: a promising formulation for the new phospholipase A2 inhibitor PX-18. Int. J. Pharm 391(1–2), 322–329. doi: 10.1016/j.ijpharm.2010.03.002 [PubMed: 20214969]

Pestel S, Martin HJ, Maier GM, Guth B, 2006. Effect of commonly used vehicles on gastrointestinal, renal, and liver function in rats. J. Pharmacol. Toxicol. Methods 54(2), 200–214. doi: 10.1016/j.vascn.2006.02.006 [PubMed: 16567111]

Savi MM, Clayton T, Furtmüller R, Gavrilovi I, Samardzi J, Savi S, Huck S, Sieghart W, Cook JM, 2008. PWZ-029, a compound with moderate inverse agonist functional selectivity at GABA(A) receptors containing alpha5 subunits, improves passive, but not active, avoidance learning in rats. Brain Res. 1208, 150–159. doi: 10.1016/j.brainres.2008.02.020 [PubMed: 18394590]

Savi MM, Majumder S, Huang S, Edwankar RV, Furtmüller R, Joksimovi S, Clayton T, Sr, Ramerstorfer J, Milinkovi MM, Roth BL, Sieghart W, Cook JM, 2010. Novel positive allosteric modulators of GABAA receptors: do subtle differences in activity at alpha1 plus alpha5 versus alpha2 plus alpha3 subunits account for dissimilarities in behavioral effects in rats?. Prog. Neuropsychopharmacol. Biol. Psychiatry 34(2), 376–386. doi: 10.1016/j.pnpbp.2010.01.004 [PubMed: 20074611]

Savi MM, Obradovi DI, Ugresi ND, Cook JM, Yin W, Van Linn M, Bokonji DR, 2006. Benzodiazepine site inverse agonists and locomotor activity in rats: bimodal and biphasic influence. Pharmacol. Biochem. Behav 84(1), 35–42. doi: 10.1016/j.pbb.2006.04.001 [PubMed: 16725185]

Sharma P, Zujovic ZD, Bowmaker GA, Marshall AJ, Denny WA, Garg S, 2011. Evaluation of a crystalline nanosuspension: polymorphism, process induced transformation and in vivo studies. Int. J. Pharm 408(1–2), 138–151. doi: 10.1016/j.ijpharm.2011.01.032 [PubMed: 21272627]

Shegokar R, Müller RH, 2010. Nanocrystals: industrially feasible multifunctional formulation technology for poorly soluble actives. Int. J. Pharm 399(1–2), 129–139. doi: 10.1016/j.ijpharm.2010.07.044 [PubMed: 20674732]

Shekunov BY, Chattopadhyay P, Tong HH, Chow AH, 2007. Particle size analysis in pharmaceutics: principles, methods and applications. Pharm. Res 24(2), 203–227. doi: 10.1007/s11095-006-9146-7 [PubMed: 17191094]

Sigfridsson K, Lundqvist A, Strimfors M, 2013. Evaluation of exposure properties after injection of nanosuspensions and microsuspenions into the intraperitoneal space in rats. Drug Dev. Ind. Pharm 39(11), 1832–1839. doi: 10.3109/03639045.2012.738684 [PubMed: 23240709]

Steckel H, Rasenack N, Villax P, Müller BW, 2003. In vitro characterization of jet-milled and in-situ-micronized fluticasone-17-propionate. Int. J. Pharm 258(1–2), 65–75. doi: 10.1016/s0378-5173(03)00153-4 [PubMed: 12753754]

Sykes E, Woodburn K, Decker D, Kessel D, 1994. Effects of Cremophor EL on Distribution of Taxol to Serum Lipoproteins. Br. J. Cancer 70(3), 401–404. doi: 10.1038/bjc.1994.317 [PubMed: 7915910]

Turner PV, Brabb T, Pekow C, Vasbinder MA, 2011. Administration of Substances to Laboratory Animals: Routes of Administration and Factors to Consider. J. Am. Assoc. Lab. Anim. Sci 50(5), 600–613.

Van Eerdenbrugh B, Van den Mooter G, Augustijns P, 2008. Top-down production of drug nanocrystals: nanosuspension stabilization, miniaturization and transformation into solid products. Int. J. Pharm 364(1), 64–75. doi: 10.1016/j.ijpharm.2008.07.023 [PubMed: 18721869]

Van Eerdenbrugh B, Vermant J, Martens JA, Froyen L, Van Humbeeck J, Augustijns P, Van den Mooter G, 2009. A screening study of surface stabilization during the production of drug nanocrystals. J. Pharm. Sci 98(6), 2091–2103. doi: 10.1002/jps.21563 [PubMed: 18803265]

Vasovi D, Divovi B, Treven M, Knutson DE, Steudle F, Scholze P, Obradovi A, Fabjan J, Brkovi B, Sieghart W, et al. , 2019. Trigeminal neuropathic pain development and maintenance in rats are suppressed by a positive modulator of α6 GABAA receptors. Eur. J. Pain 23(5), 973–984. doi: 10.1002/ejp.1365 [PubMed: 30633839]

Wang L, Du J, Zhou Y, Wang Y, 2017. Safety of nanosuspensions in drug delivery. Nanomedicine 13(2), 455–469. doi: 10.1016/j.nano.2016.08.007 [PubMed: 27558350]

Wang Y, Zheng Y, Zhang L, Wang Q, Zhang D, 2013. Stability of nanosuspensions in drug delivery. J. Control. Release 172, 1126–1141. doi: 10.1016/j.jconrel.2013.08.006 [PubMed: 23954372]

Williams HD, Trevaskis NL, Charman SA, Shanker RM, Charman WN, Pouton CW, Porter CJ, 2013. Strategies to address low drug solubility in discovery and development. Pharmacol. Rev 65(1), 315–499. doi: 10.1124/pr.112.005660 [PubMed: 23383426]

Wu L, Zhang J, Watanabe W, 2011. Physical and chemical stability of drug nanoparticles. Adv. Drug Deliv. Rev 63(6), 456–469. doi: 10.1016/j.addr.2011.02.001 [PubMed: 21315781]

Xu Y, Liu X, Lian R, Zheng S, Yin Z, Lu Y. and Wu W, 2012. Enhanced dissolution and oral bioavailability of aripiprazole nanosuspensions prepared by nanoprecipitation/homogenization based on acid–base neutralization. Int. J. Pharm 438(1–2), 287–295. doi: 10.1016/j.ijpharm.2012.09.020 [PubMed: 22989976]

Yang H, Teng F, Wang P, Tian B, Lin X, Hu X, Zhang L, Zhang K, Zhang Y, Tang X, 2014. Investigation of a nanosuspension stabilized by Soluplus® to improve bioavailability. Int. J. Pharm 477(1–2), 88–95. doi: 10.1016/j.ijpharm.2014.10.025 [PubMed: 25455766]

Zhang Z, Tan S, Feng SS, 2012. Vitamin E TPGS as a molecular biomaterial for drug delivery. Biomaterials 33(19), 4889–4906. doi: 10.1016/j.biomaterials.2012.03.046 [PubMed: 22498300]

Zuidema J, Kadir F, Titulaer HAC, Oussoren C, 1994. Release and absorption rates of intramuscularly and subcutaneously injected pharmaceuticals (II). Int. J. Pharm 105(3), 189–207. doi: 10.1016/0378-5173(94)90103-1
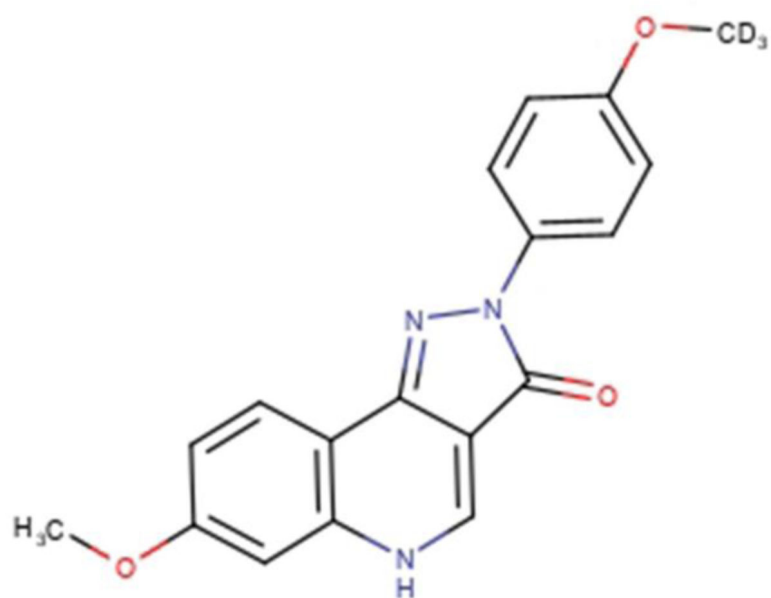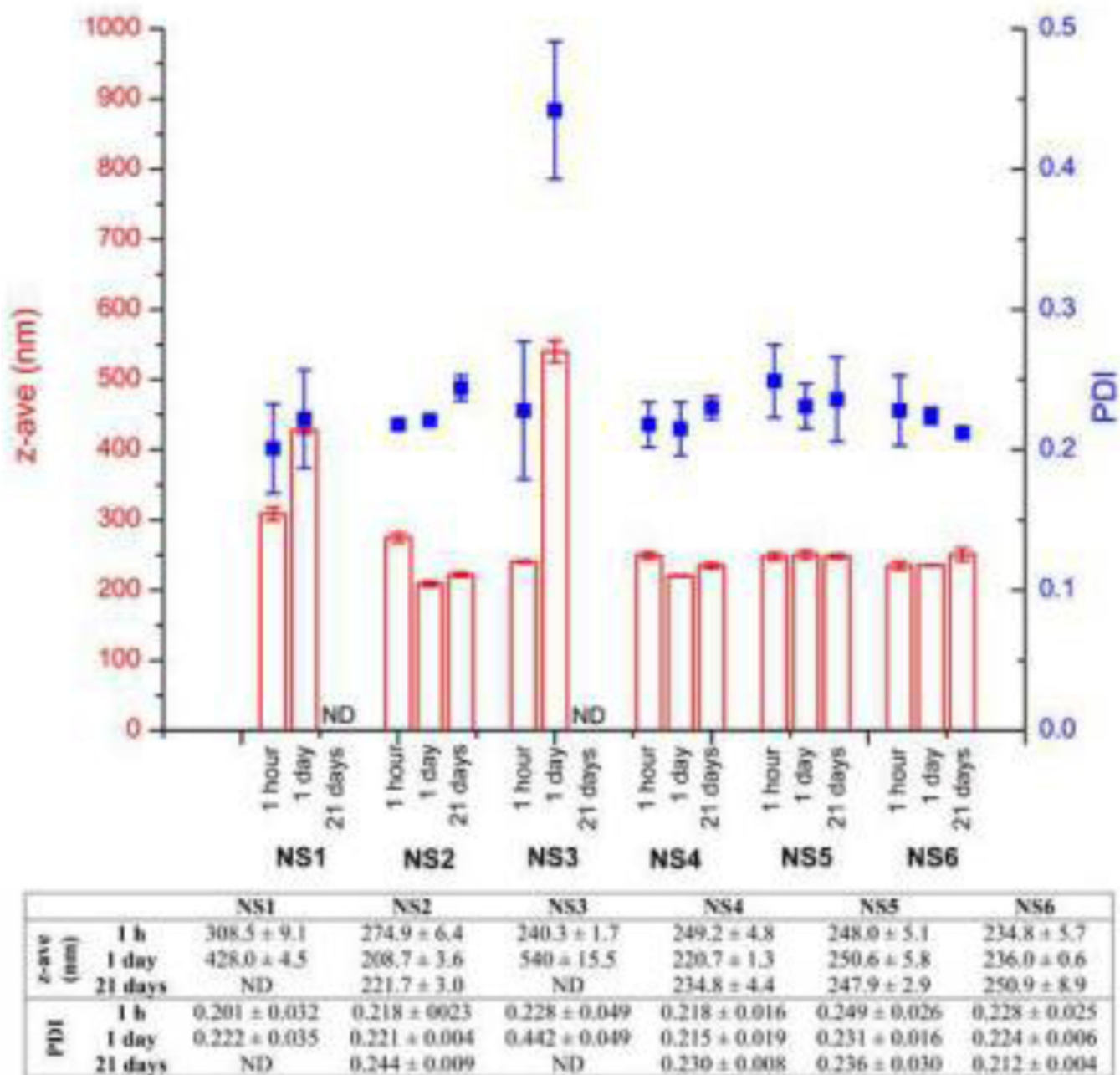
Figure 1.
The chemical structure of DK-I-56–1.

		NS1	NS2	NS3	NS4	NS5	NS6
z-ave (nm)	1 h	308.5 ± 9.1	274.9 ± 6.4	240.3 ± 1.7	249.2 ± 4.8	248.0 ± 5.1	234.8 ± 5.7
	1 day	428.0 ± 4.5	208.7 ± 3.6	540 ± 15.5	220.7 ± 1.3	250.6 ± 5.8	236.0 ± 0.6
	21 days	ND	221.7 ± 3.0	ND	234.8 ± 4.4	247.9 ± 2.9	250.9 ± 8.9
PDI	1 h	0.201 ± 0.032	0.218 ± 0023	0.228 ± 0.049	0.218 ± 0.016	0.249 ± 0.026	0.228 ± 0.025
	1 day	0.222 ± 0.035	0.221 ± 0.004	0.442 ± 0.049	0.215 ± 0.019	0.231 ± 0.016	0.224 ± 0.006
	21 days	ND	0.244 ± 0.009	ND	0.230 ± 0.008	0.236 ± 0.030	0.212 ± 0.004

Figure 2.
Mean hydrodynamic diameter (z-ave) and polydispersity index (PDI) of prepared nanosuspensions (NS1-NS6); ND – not determined. $P < 0.05$, z-ave: NS1 – 1 h vs. 1 day; NS2 – 1 h vs. 1 day, 1 h vs. 21 days, 1 day – 21 days; NS3 – 1 h vs. 1 day; NS4 – 1 h vs. 1 day, 1 h vs. 21 days; NS6 – 1 h vs. 21 days; PDI: NS3 – 1 h vs. 1 day.
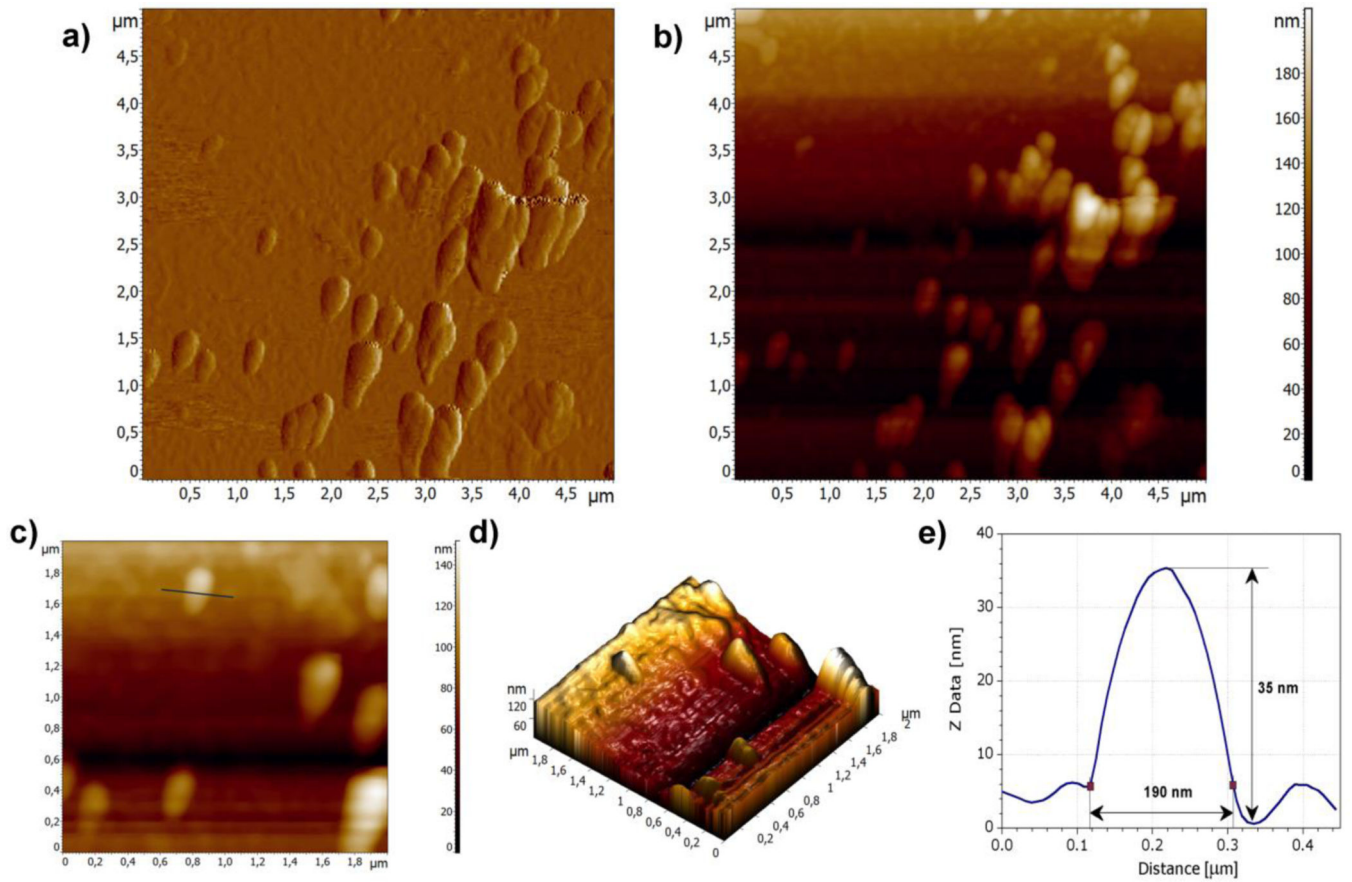
Figure 3.
AFM images of diluted NS2 sample: (a) error signal of 5×5 μm area of the sample; (b) 2D topography of 5×5 μm area of the sample; (c) 2D topography of 2×2 μm area of the sample with the marked line along which the profile was obtained; (d) 3D topography of 2×2 μm area of the sample; and (e) height profile of the selected particle.

Figure 4.
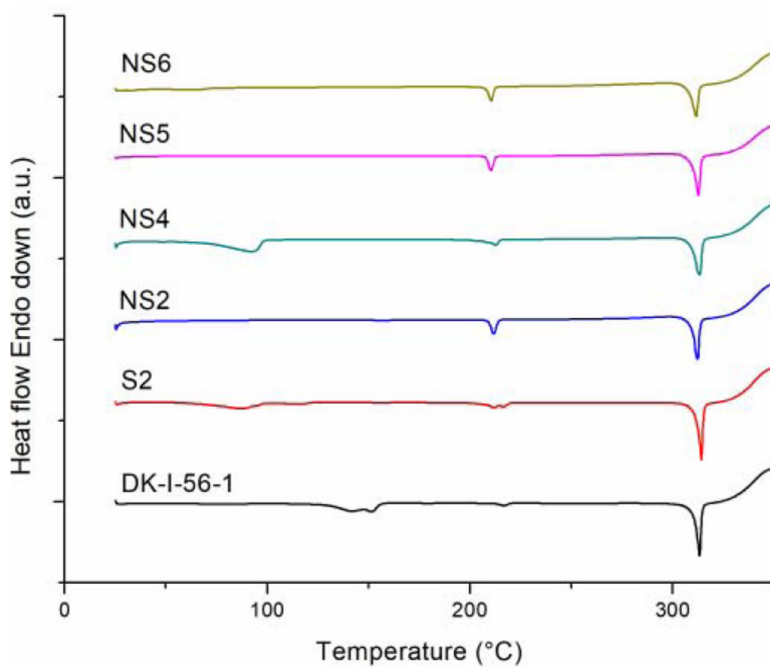DSC thermogram of unprocessed DK-I-56–1, suspension (S2) and selected nanosuspension formulations (NS2, NS4, NS5 and NS6).
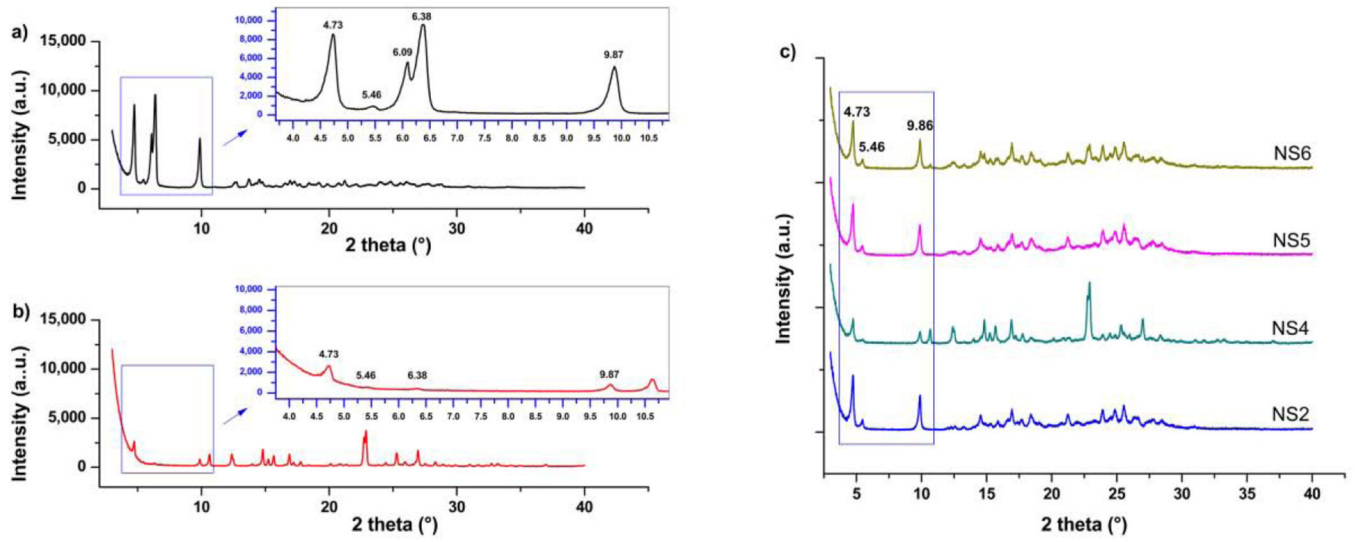
Figure 5.
XRPD patterns of unprocessed (a) DK-I-56–1, (b) suspension (S2) and (c) selected
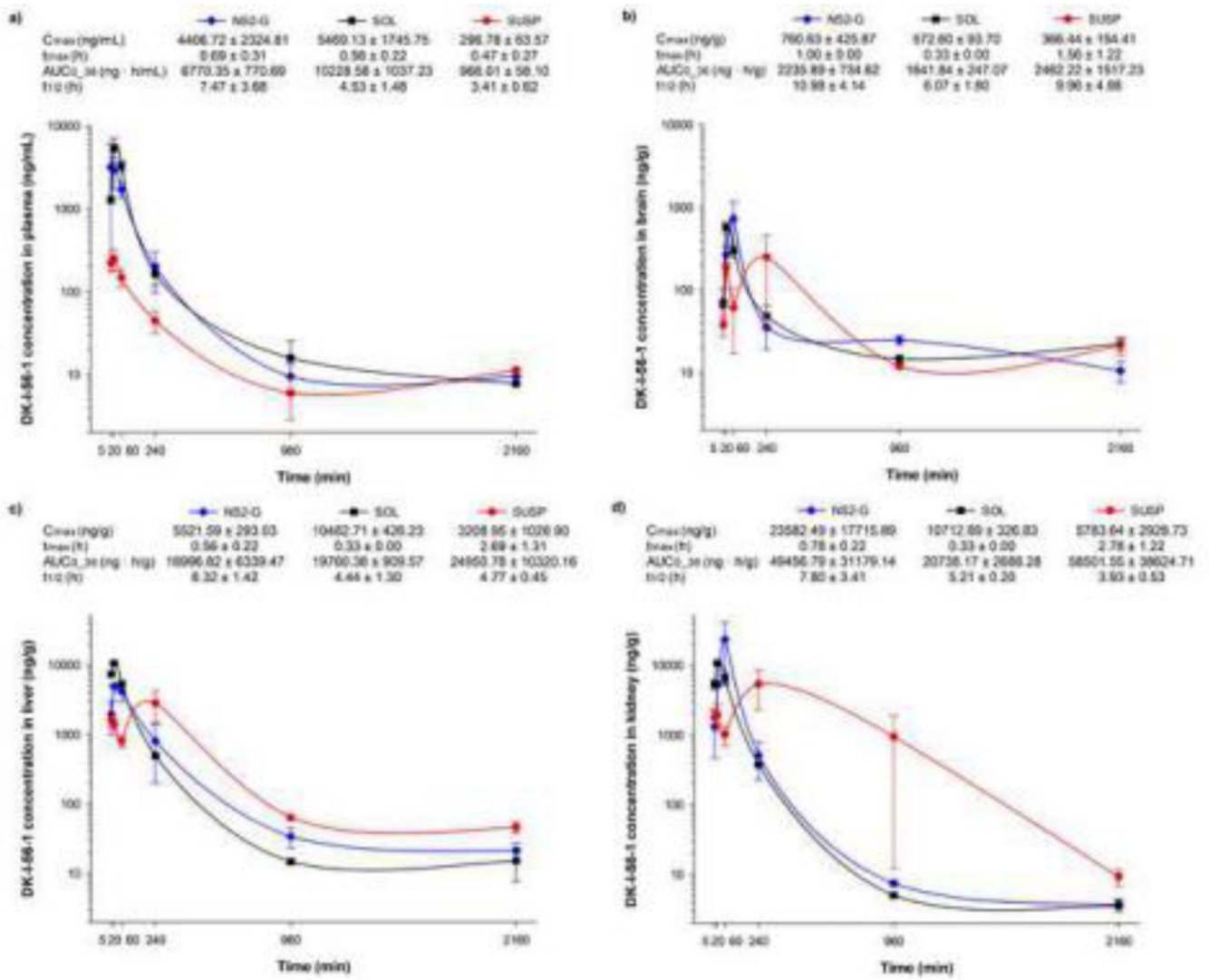nanosuspension formulations (NS2, NS4, NS5 and NS6).

Figure 6.
Pharmacokinetic profiles and calculated parameters of nanosuspension (NS2-G), suspension (SUSP) and solution (SOL) in (a) plasma, (b) brain, (c) liver and (d) kidney after intraperitoneal administration in mice (n = 3 per time point) at dose of 10 mg/kg. C_{max} – maximum concentration; t_{max} – time of maximum concentration; AUC_{0-36} – area under the concentration versus time curve from zero to last measurable time point; $t_{1/2}$ - terminal elimination half-life.
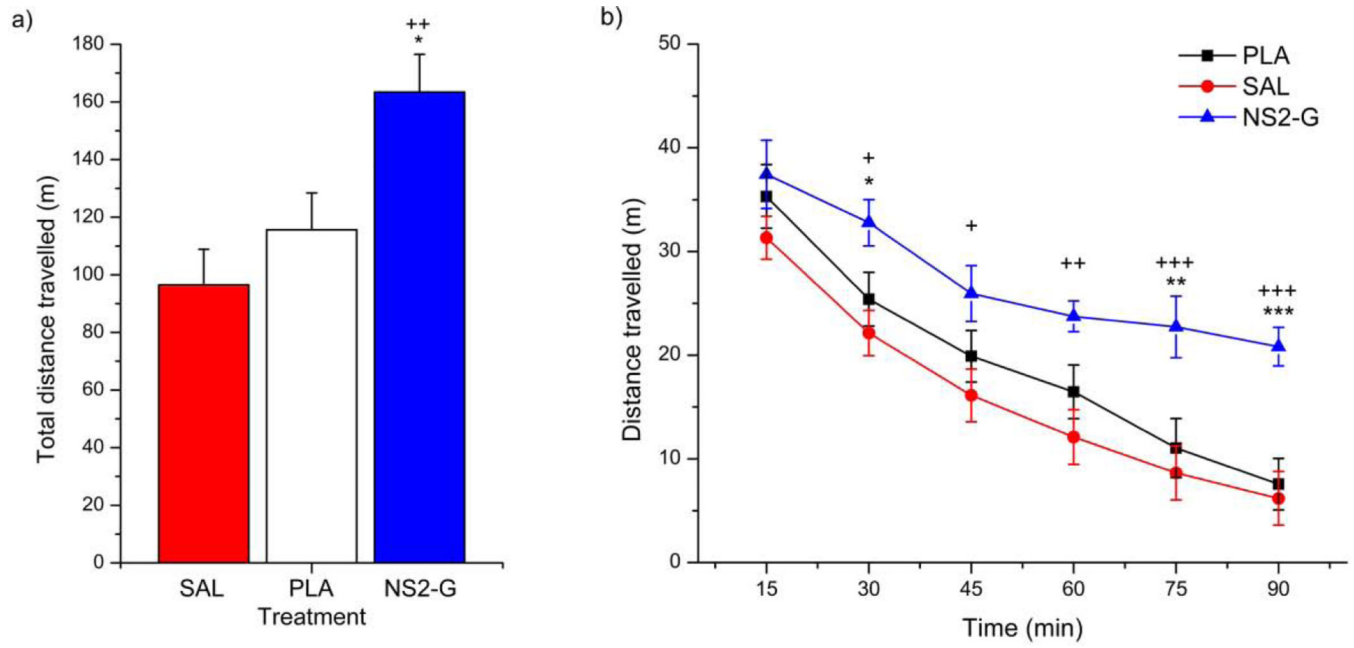
Figure 7.
Effects of nanosuspension (NS2-G) on (a) total distance travelled and (b) distance travelled
in mice. Data are presented as mean ± S.E.M. Post hoc significant differences are as follows:
*, ** and ***, $P < 0.05$; $P < 0.01$ and $P < 0.001$ vs. PLA; +, ++ and +++, $P < 0.05$; $P < 0.01$
and $P < 0.001$ vs. SAL; SAL- saline, PLA – placebo.

Table 1.

Solubility of DK-I-56–1 in selected excipients (mean ± S.D, n=3).

Solvent	Solubility (mg/ml)
Water (pH 5.2)	0.0063 ± 0.0007
Isopropanol	1.0347 ± 0.0230
Methanol	0.7957 ± 0.1206
Ethanol, 70% v/v	1.1574 ± 0.0564
Dimethyl sulfoxide	137.9516 ± 2.8977
Medium chain triglycerides	0.0987 ± 0.0053
Soybean oil	0.0392 ± 0.0010
Castor oil	0.5379 ± 0.0516
Fish oil	0.0255 ± 0.0010
Benzyl alcohol	7.7999 ± 0.6036